Leveraging domain adaptation for efficient seismic denoising

Claire Birnie and Tariq Alkhalifah, King Abdullah University of Science and Technology (KAUST)

SUMMARY

The selection of training data for deep learning procedures dictates both the neural network's performance and its applicability to further datasets. Particularly in seismic applications, the selection is non-trivial with the common approaches of manually labelling field data or generating synthetic data both exhibiting severe limitations. The former in its inability to outperform conventional approaches required for the label generation and the later in its inability to properly represent future application data. Domain adaptation, through input features and label transformations, offers the potential to leverage on the benefits of both these approaches while reducing their drawbacks. In this work we illustrate how vital information from field data can be incorporated into a training procedure on synthetic data with the trained network successfully applied on the field data afterwards, despite large differences between the training and inference, i.e., synthetic and field, datasets. Furthermore, we illustrate how an inverse correlation procedure can be incorporated into the training procedure in an attempt to maintain the original wavefield properties.

INTRODUCTION

How best to generate training data for Machine Learning (ML) applications is a question that plagues the geophysics community. Due to their data-driven nature, it is of paramount importance that ML algorithms are trained on data with the same properties and distribution as they are going to be applied on. Within the geophysics community two main approaches are taken for selecting training data: label field data or generate synthetic training data.

Labelling field data has the huge benefit that the data onto which the network is trained is likely of the same characteristics onto which the network will be applied in the future. However, it also comes with the drawback of how to generate the 'labels'. For instance, in the denoising setting, the labels should be the clean waveform data however to generate that from field data we are currently restricted to the denoising performance of our conventional denoising algorithms, such as FK-deconvolution or curvelets. In the end, using such an approach to generate the labels results in a Neural Network (NN) that can only perform, at best, as well as our conventional denoising algorithms although, perhaps with more computational efficiency.

The use of synthetic data sets for training overcomes this hurdle, allowing a completely noise-free label to be generated for the training procedure. However, the challenge of generating realistic synthetic datasets is well documented with multiple studies illustrating the danger of using non-realistic synthetic datasets. A great deal of effort has been expended on determining how best to create realistic synthetic datasets focusing on both subsurface properties and noise settings, for example Bakulin and Silvestrov (2021) and Birnie et al. (2020), respectively. A number of studies have chosen to forgo noise modelling completely and instead add recorded field noise onto modelled waveform data, generating so-called semi-synthetics (e.g., Mousavi et al., 2019; Wang et al., 2021). Despite these advancements, it is still unclear to what extent our waveforms and noise imitate field data, and, in extension, how our trained NN procedures will perform when applied to field data.

Finally, there are a number of works that have concluded it is better to circumvent the requirement for noisy-clean training datasets by utilising unsupervised or self-supervised procedures, for example Zhang et al. (2019) and Birnie et al. (2021) respectively. However, within the wider computer-vision field, it has been shown that such procedures do not perform as well as their supervised counterparts (Krull et al., 2019).

Recent work by Alkhalifah et al. (2021) introduced MLReal - a domain adaptation (Kouw and Loog, 2019) procedure that allows for inclusion of the field data's properties into the training cycle whilst using a synthetic data for training. By convolving training data patches with random patches of field data, the network is exposed to the characteristics of the field data without requiring any labels on the field dataset. In this work, we build on the work of MLReal by adapting the workflow for preservation of the wavefields' properties, therefore extending the applicability of MLReal to scenarios in which the wavefield should remain unchanged, such as denoising. We apply this modified framework on a denoising task.

METHODOLOGY

In this work we adapt the previous workflow of MLReal to ensure that the wavefield properties are preserved. To do so, we implement an inverse correlation step on the product of the neural network. This updated workflow is illustrated in Figure 1.

The training procedure is largely implemented on the labelled synthetic data. Prior to input in the NN, each patch of synthetic data is cross-correlated with a single reference trace extracted from the data patch. Inside the training loop, for each epoch a random patch of field data is selected, auto-correlated on a trace-by-trace basis and convolved with each of the cross-correlated synthetic data patches - this becomes the input to the network. The target of the network is the equivalent of the clean synthetic waveform being cross-correlated with the reference traces. Therefore, to return the NN prediction to the original wavefield properties (e.g., onset time and amplitude) the NN output undergoes an inverse correlation stage.

The inverse correlation is computed in the frequency domain as follows:

$$\tilde{X}(f) = \frac{Y(f)}{H^*(f)} \cdot \frac{H(f)}{H(f)} = \frac{Y(f)H(f)}{|H(f)|^2 + \varepsilon} \tag{1}$$

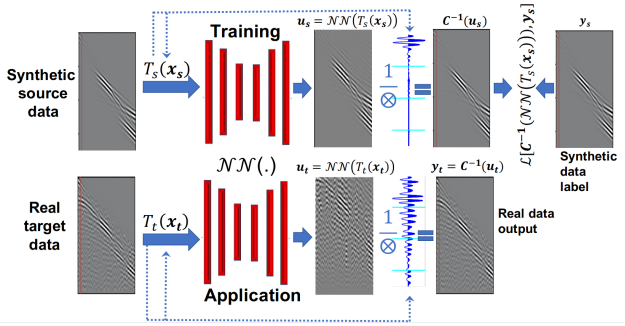

Figure 1: Adaptation of the MLReal workflow to retain temporal information through the inclusion of an inverse correlation step. (Adapted from Alkhalifah et al. (2021))

where $\tilde{X}(f)$ is the estimated decorrelated trace in frequency domain, $Y(f)$ is the correlated trace in frequency domain (output of the neural network) and $H(f)$ is the reference trace in frequency domain. $H^*(f)$ denotes the complex conjugate of reference trace in F-domain while ε is a water-level used for stabilising the inverse correlation function. In this work, we investigated the role of ε and found that an optimum value is given by $1e-2$.

After the inverse correlation step, the output should ideally equal the clean synthetic wavefield data. To enforce this requirement, the loss function is computed on the product of the inverse correlation compared with the clean wavefield data, as opposed to computing the loss directly on the NN prediction and comparing it to the wavefield data cross-correlated with the patches' reference traces. We found this to also help reduce the introduction of instability in the inverse correlation step due to prediction errors arising from the network.

For the inference workflow, the real data undergoes a similar pre-processing procedure as the synthetic data did during the training stage. However, at this stage, once the field data patches cross-correlated with their reference traces, these patches are convolved with a patch that is the average of the auto-correlation of all the synthetic training patches. Then, as before, the cross-correlated, convolved patches are input into the network and then the inverse correlation procedure is computed on the network's prediction.

RESULTS

In the preliminary stages of this research we solely focus on synthetic datasets to allow in-depth analysis on the performance of the denoising procedure. To imitate the synthetic and field data described in the methodology we introduce different noise settings into the datasets, while retaining the same underlying wavefield data. For the 'synthetic' training data we use coloured, Gaussian noise that has been filtered with respect to both space and time with a filter length of two. For the 'field' inference data we generate semi-synthetics, i.e., combine modelled waveforms with recorded field noise, using the same noise as previously used by Wang et al. (2021).

We train a 4-layer, UNet-style network containing residual blocks, as opposed to the traditional convolutional blocks utilised by Ronneberger et al. (2015). The network has 32 initial filters increasing by a factor of two per layer, resulting in $\sim 106M$ trainable parameters. The network is trained over 150 epochs with 8092 training samples and 1024 validation samples, of patch size 64×64.

Figure 2 illustrates the performance of the trained network when applied to the training data. As a reminder, the training data has been cross-correlated with a reference trace prior to being convolved with a random sample from the inference data that has undergone a trace-by-trace auto-correlation. For each panel in Figure 2, the top row shows the true data, while the second row represents the network's prediction and finally, the bottom row highlights the differences between the true and predicted values. It can be seen that for both these example patches a significant volume of noise has been suppressed while the decorrelated product of the network's prediction is very similar to the clean waveform target. There are some large errors in the correlated label and the network's prediction. However these errors have been significantly reduced during the inverse correlation step, with only a small amount of signal leakage observable in the difference plots.

Finally, Figure 3 illustrates the trained network when applied as part of the inference pipeline. As a reminder, as opposed to convolving with a random, auto-correlated patch as done in training, during the inference procedure the field data patches are convolved with the mean of the auto-correlation of all the synthetic training patches. It is important to note here that the network has not fully seen these data patches during training, as they are synonymous to field data, therefore the target is purely for visualisation purposes and not used in the training or prediction stages. Similar to the results on the training data, it can be observed that the network hasn't accurately predicted the correlated, clean waveform data (middle column of each panel). However, these large errors have been absorbed in the inverse correlation step resulting in minimal differences between the target data and the decorrelated NN product (fourth column of each panel). Therefore, the trained network has efficiently suppressed almost all the field noise in the inference data.

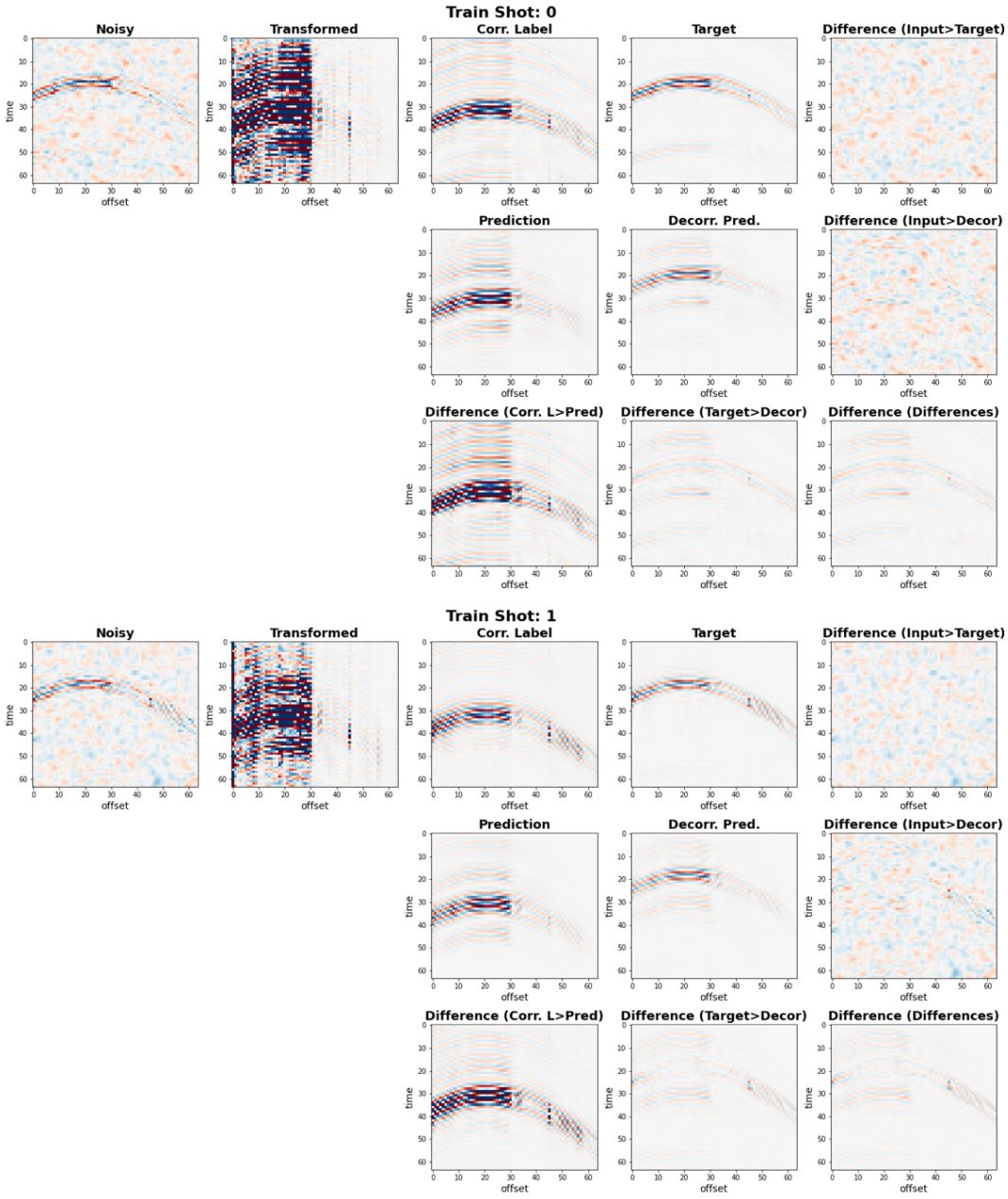

Figure 2: Results from MLReal denoising applied to the synthetic training dataset contaminated with coloured, Gaussian noise. In the two shot panels, the top row represents the ground truth; the second row illustrates the output of the workflow at the NN prediction stage, the product of the inverse correlation and the difference between the original noisy data and the decorrelated prediction; and, the bottom row highlights the differences between the ground truth and MLReal predictions.

DISCUSSION AND CONCLUSIONS

In this work, we have illustrated how the MLReal domain adaptation workflow can be extended to allow for retention of the wavefields' properties and thereby expanding it's field of applicability to a whole host of processing tasks, such as denoising, multiple attenuation, and wavefield separation, to name a few. The inclusion of the inverse correlation step makes this possible, however it is a process that is known to be highly unstable. Therefore, to improve its stability the inverse correlation step has been incorporated into the training procedure leveraging PyTorch's Fast Fourier Transform, allowing the loss to be computed after the inverse correlation and the resulting errors to be back-propagated through both the inverse correlation and the NN.

Furthermore, we used noise with significantly different characteristics to represent the synthetic and field datasets, i.e.,

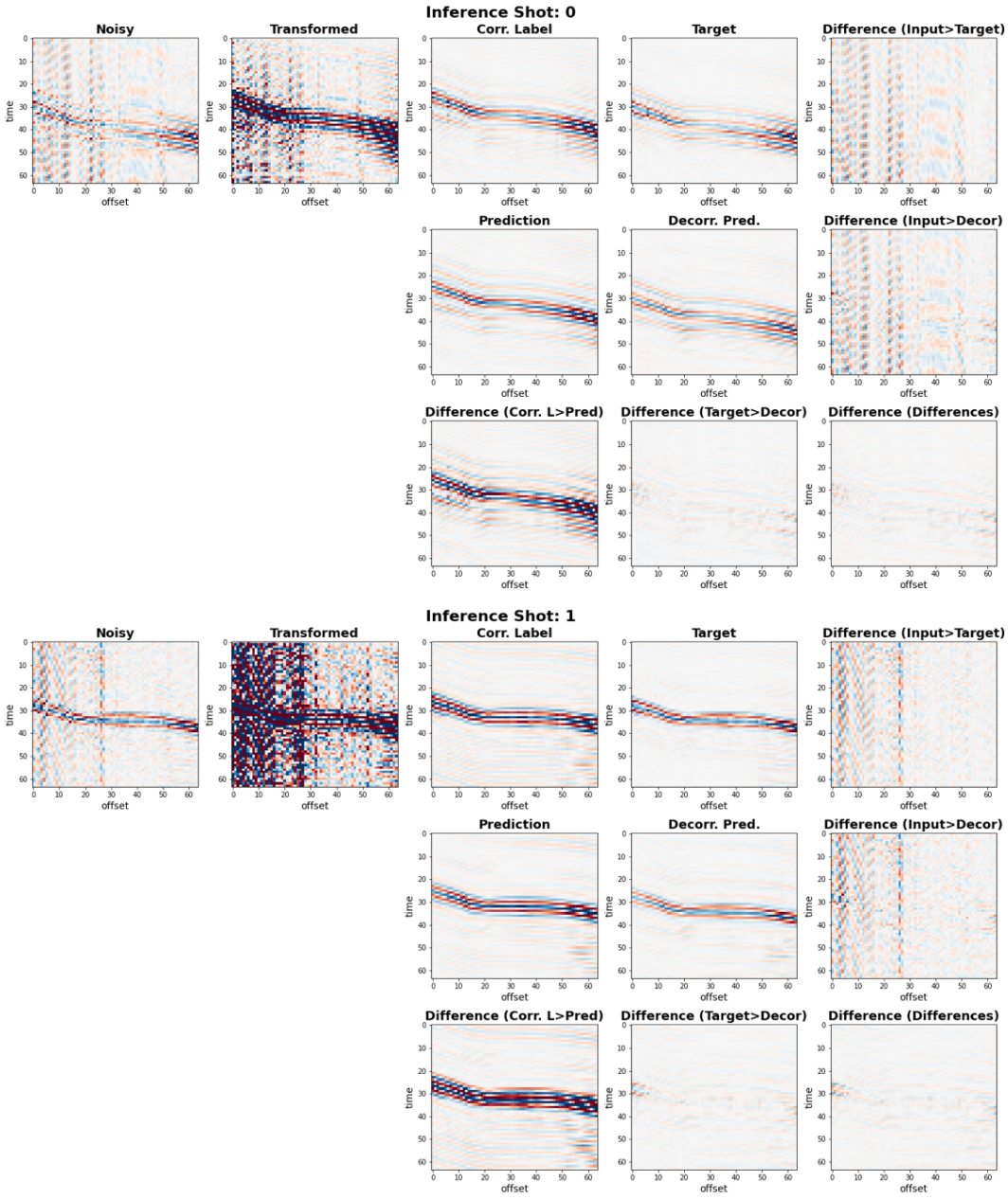

Figure 3: Results from MLReal denoising applied to the semi-synthetic inference dataset. In the two shot panels, the top row represents the ground truth; the second row illustrates the output of the workflow at the NN prediction stage, the product of the inverse correlation and the difference between the original noisy data and the decorrelated prediction; and, the bottom row highlights the differences between the ground truth and MLReal predictions.

random, coloured noise vs. field noise with strong spatio-temporal coherency. The successful application of the trained network highlights the potential of domain adaptation as a way to overcome the challenge of generating realistic synthetic datasets, whilst also avoiding the requirement of labelling field data. Future work shall focus not only on progressing this work to field data, but also extending the technique to patch-based denoising, a common approach for denoising large seismic sections and volumes.

ACKNOWLEDGMENTS

The authors thank Prof. M. Ravasi, Dr O. Ovcharenko and Dr H. Wang for insightful discussions, as well as the wider KAUST Seismic Wave Analysis Group. For computer time, this research used the resources of the Supercomputing Laboratory at King Abdullah University of Science & Technology (KAUST) in Thuwal, Saudi Arabia.

REFERENCES

Alkhalifah, T., H. Wang, and O. Ovcharenko, 2021, Mlreal: Bridging the gap between training on synthetic data and real data applications in machine learning: 82nd EAGE Annual Conference & Exhibition, European Association of Geoscientists & Engineers, 1–5.

Bakulin, A., and I. Silvestrov, 2021, Understanding acquisition and processing challenges in the desert environment through seam arid and barrett models: Presented at the SEG/AAPG/SEPM First International Meeting for Applied Geoscience & Energy, OnePetro.

Birnie, C., K. Chambers, D. Angus, and A. L. Stork, 2020, On the importance of benchmarking algorithms under realistic noise conditions: Geophysical Journal International, **221**, 504–520.

Birnie, C., M. Ravasi, S. Liu, and T. Alkhalifah, 2021, The potential of self-supervised networks for random noise suppression in seismic data: Artificial Intelligence in Geosciences.

Kouw, W., and M. Loog, 2019, A review of domain adaptation without target labels: IEEE Transactions on Pattern Analysis and Machine Intelligence, **PP**, 1–1.

Krull, A., T.-O. Buchholz, and F. Jug, 2019, Noise2void-learning denoising from single noisy images: Proceedings of the IEEE/CVF Conference on Computer Vision and Pattern Recognition, 2129–2137.

Mousavi, S. M., W. Zhu, Y. Sheng, and G. C. Beroza, 2019, Cred: A deep residual network of convolutional and recurrent units for earthquake signal detection: Scientific reports, **9**, 1–14.

Ronneberger, O., P. Fischer, and T. Brox, 2015, U-net: Convolutional networks for biomedical image segmentation: International Conference on Medical image computing and computer-assisted intervention, Springer, 234–241.

Wang, H., T. Alkhalifah, U. bin Waheed, and C. Birnie, 2021, Data-driven microseismic event localization: an application to the oklahoma arkoma basin hydraulic fracturing data: IEEE Transactions on Geoscience and Remote Sensing.

Zhang, M., Y. Liu, and Y. Chen, 2019, Unsupervised seismic random noise attenuation based on deep convolutional neural network: IEEE Access, **7**, 179810–179822.